

# Structural health monitoring of seismically vulnerable RC frames under lateral cyclic loading

Constantin E. Chalioris\*, Maristella E. Voutetaki<sup>2a</sup> and Angelos A. Liolios<sup>1b</sup>

<sup>1</sup>Department of Civil Engineering, School of Engineering, Democritus University of Thrace, Xanthi 67100, Greece

<sup>2</sup>Department of Architectural Engineering, School of Engineering, Democritus University of Thrace, Xanthi 67100, Greece

(Received March 25, 2020, Revised May 20, 2020, Accepted June, 10, 2020)

**Abstract.** The effectiveness and the sensitivity of a Wireless impedance/Admittance Monitoring System (WiAMS) for the prompt damage diagnosis of two single-storey single-span Reinforced Concrete (RC) frames under cyclic loading is experimentally investigated. The geometrical and the reinforcement characteristics of the RC structural members of the frames represent typical old RC frame structure without consideration of seismic design criteria. The columns of the frames are vulnerable to shear failure under lateral load due to their low height-to-depth ratio and insufficient transverse reinforcement. The proposed Structural Health Monitoring (SHM) system comprises of specially manufactured autonomous portable devices that acquire the in-situ voltage frequency responses of a network of twenty piezoelectric transducers mounted to the RC frames. Measurements of external and internal small-sized piezoelectric patches are utilized for damage localization and assessment at various and increased damage levels as the magnitude of the imposed lateral cycle deformations increases. A bare RC frame and a strengthened one using a pair of steel crossed tension-ties (X-bracing) have been tested in order to check the sensitivity of the developed WiAMS in different structural conditions since crack propagation, damage locations and failure mode of the examined frames vary. Indeed, the imposed loading caused brittle shear failure to the column of the bare frame and the formation of plastic hinges at the beam ends of the X-braced frame. Test results highlighted the ability of the proposed SHM to identify incipient damages due to concrete cracking and steel yielding since promising early indication of the forthcoming critical failures before any visible sign has been obtained.

**Keywords:** reinforced concrete (RC) frame; structural health monitoring (SHM); lateral cyclic testing; seismic vulnerability; shear; piezoelectric lead zirconate titanate (PZT); damage assessment

## 1. Introduction

Recent earthquakes in the eastern Mediterranean countries highlighted that shear brittle failure of Reinforced Concrete (RC) column in existing frame structures, particularly built with old Code Standards, poses a serious seismic risk. Earthquake damages in critical RC members adversely impact the ability of structures to withstand future seismic excitations and increase risk to fatal failures and catastrophic collapses if not controlled. Thus, the real time surveillance, the continuous inspection and the in-situ measurements of efficient Structural Health Monitoring (SHM) techniques help to ensure continuous life-safety, functional and economical operation of these buildings. Prompt damage diagnosis of seismically vulnerable buildings is a current necessity in earthquake prone areas (Rainieri *et al.* 2011, Kong *et al.* 2016).

The majority of the existing RC buildings in most of the eastern Mediterranean countries were designed and constructed according to older Codes with inadequate

seismic requirements regarding the provisions of modern Code Standards. Many of these structures have insufficient reinforcement, morphological problems such as soft storey, short columns, lack of strong RC walls, weak column strong beam frames, etc., and low quality of building materials. Apparently, the structural members of such RC buildings present weaknesses concerning their strength, ductility and stiffness in earthquakes (Tsonos 2002, Lagaros *et al.* 2006, Favvata and Karayannis 2009, Sharma *et al.* 2012, Karayannis *et al.* 2013, Lima *et al.* 2017, Karayannis and Naoum 2018, Kalogeropoulos and Tsonos 2020). Seismic upgrading in this type of structures is essential in order to avoid sudden total or local collapses, excessive damages or even loss of life from earthquakes. However, proper strengthening works is a complex, highly labour intensive, time-consuming and usually expensive process that is difficult to be widely applied in the majority of the existing seismically vulnerable RC structures (Tsonos 2001, 2008, Tsonos and Stylianidis 2002, Karayannis and Sirkelis 2002, Karayannis *et al.* 2008, 2018, Vougioukas *et al.* 2005, Kalogeropoulos and Tsonos 2014, Tsonos *et al.* 2017, Kalogeropoulos *et al.* 2018, Chalioris *et al.* 2018, Ganesh and Murthy 2019, Kota *et al.* 2019, Kuntal *et al.* 2020).

Recent developments in SHM techniques increased the efficiency of structural integrity assessment procedures and reduced the cost and the complexity in continuous real-time monitoring of large-scale structures. Modern monitoring

\*Corresponding author, Ph. D. Associate Professor  
E-mail: [chaliori@civil.duth.gr](mailto:chaliori@civil.duth.gr)

<sup>a</sup>Ph.D. Assistant Professor

<sup>b</sup>Ph.D.

systems utilize the Electro-Mechanical Impedance (EMI) sensing method that has been proved as a promising technique for the continuous inspection and damage assessment of existing in-service infrastructures. EMI technique is distinguished by its capability of capturing a wide range of structural damage, implementation simplicity, no interruption to the service of the structure, availability of continuous on-line monitoring and use of low-cost Piezoelectric of lead Zirconate Titanate (PZT) transducers (Park *et al.* 2000, Na and Lee 2012).

The attractive features of small size, wide bandwidth and dual function in sensing and actuating of the PZTs have recently been investigated in the field of SHM techniques (Kaur and Bhalla 2015, Vega *et al.* 2019, Shin and Oh 2009, Yang *et al.* 2010, Wang and Zhu 2011). EMI method is exploiting these merits along with the mechanical interaction between the PZTs and the infrastructure which host these piezoelectric transducers. Particularly, PZT actuators are excited by the application of an input harmonic voltage to mechanical vibration which is transmitted as a mechanical wave to the material of the structure under inspection due to the strong interfacial bonding characteristics. The mechanical response of the host structural member to this wave is received back from the PZT sensor feedback output electrical signal (Wang *et al.* 2013, Providakis and Liarakos 2014).

Several researches have been conducted on RC using the EMI method with the majority of the work being focused on SHM and damage detection in plain concrete (Vega *et al.* 2019, Shin and Oh 2009, Yang *et al.* 2010, Wang and Zhu 2011, Wang *et al.* 2013, Providakis and Liarakos 2014, Narayanan and Subramaniam 2016, Ai *et al.* 2016, Tian *et al.* 2017, Liu *et al.* 2017, Talakokula *et al.* 2018, Ghafari *et al.* 2018) steel reinforcing bars (Karayannis *et al.* 2015, 2016), bond development at the steel-concrete interface (Tawie and Lee 2010, Xu *et al.* 2013), steel fibre reinforced concrete (Kang *et al.* 2018) and RC members subjected to corrosion (Talakokula *et al.* 2014, Talakokula and Bhalla 2015) and monotonic loads (Karayannis *et al.* 2016, Soh *et al.* 2009, Song *et al.* 2007, 2008, Divsholi *et al.* 2009, Hu *et al.* 2014, Divsholi and Yang 2014, Chalioris *et al.* 2015a, Voutetaki *et al.* 2016, Ai *et al.* 2018, 2019). Concerning the seismic risk, there are only a few published works that deal with the monitoring of shear and seismic compressive stress in concrete (Hou *et al.* 2012, 2013), shaking table test of an one-bay-two-storey RC frame (Hou *et al.* 2017), the dynamic modeling of embeddable PZTs (Huo *et al.* 2017) and the damage assessment of seismically valuable RC members under dynamic loading or lateral imposed cyclic deformations (Bhalla S, Soh 2004, Laskar *et al.* 2009, Gu *et al.* 2010, Chalioris *et al.* 2015b, 2016, Zhang *et al.* 2018).

Recently, a new PZT-based active sensing Wireless impedance/Admittance Monitoring System (WiAMS) has been developed by Providakis *et al.* (2014a, b, 2016). The control unit of this SHM system uses the low-cost, small-sized and powerful single-board computer Raspberry PI. Autonomous portable WiAMS devices are cable connected with piezoelectric transducers that are properly mounted to the RC structural members in order to control the PZTs

actuating/sensing functions from a distance and to perform real-time and continuous structural integrity assessment. Applications of the proposed SHM system in RC beams have shown promising results concerning its effectiveness to detect concrete cracking and steel reinforcing yielding in early damage levels (Karayannis *et al.* 2015, 2016, Chalioris *et al.* 2015a, 2015b, 2016, Voutetaki *et al.* 2016).

The feasibility of the wireless PZT-based SHM system for concrete members proposed by Providakis *et al.* (2014a, b, 2014c, 2016) and experimentally validated by the authors in monotonically tested RC beams (Karayannis *et al.* 2015, 2016, Chalioris *et al.* 2015a, Voutetaki *et al.* 2016) is further validated herein for the prompt damage diagnosis of seismically deficient single-storey single-span RC frames subjected to lateral cyclic loading. Dimensions and reinforcement configuration of the frames represent typical old RC frame structures which are vulnerable to brittle catastrophic failure during seismic excitations. Such structures usually appear typical shear character deficiencies due to the inadequate confining - transverse reinforcement and the short height of the columns. Damage localization and assessment at various and increased damage levels as the magnitude of the imposed cycle deformations increases is also attempted herein using the in-situ voltage measurements of a network of PZTs that have been mounted to the frames using three different types of installation.

The experimental program of this research includes two large-scale RC frame specimens; a bare frame (reference specimen) and an X-braced frame that has the same RC structural characteristics with the bare one and it has also been strengthened using a pair of steel crossed tension-ties. Thus, the damage propagation and the failure mode of the examined RC frames are expected to be varied. This way, the sensitivity of the proposed wireless monitoring system to detect, identify and quantify different types of induced damages at various locations and structural conditions would be checked.

## 2. Orientation of the developed monitoring system

The Structural Health Monitoring (SHM) system used in this experimental study is based on the Electro-Mechanical Impedance (EMI) sensing method utilizing the voltage signal measurements of a series of Piezoelectric of lead Zirconate Titanate (PZT) transducers mounted to the tested RC frames. The main aspects and the developed device of this integrated damage diagnosis technique are presented in the following subsections.

### 2.1 Numerical simulation procedure

EMI-based SHM methods utilize piezoelectric patches that are properly mounted to an infrastructure by robust bonding interface in order to operate as (a) actuators to vibrate the inspection area of the structure in terms of mechanical wave with high frequency excitations (converse piezoelectric effect), and simultaneously as (b) sensors to monitor the changes in their electrical impedance due to the

mechanical reaction wave, or else to the mechanical impedance of the structure (direct piezoelectric effect).

The PZT transducers are compact, lightweight, small-sized and exhibit excellent SHM characteristics, such as large range of linearity, self-sensing, fast response, low-cost, high conversion efficiency and long-term stability. The following theoretical aspect is considered in the developed monitoring system. The voltage across the direction of the width axis of the PZT,  $V_{pzt(t)}$ , is expressed as a function of time,  $t$ , of an input sinusoidal voltage signal:

$$V_{pzt}(t) = V_p \sin(2\pi ft) \quad (1)$$

where  $V_p$  is the peak voltage of the signal and  $f$  is the frequency (Hz).

The current signal of the PZT,  $I_{pzt(t)}$ , is also expressed as a function of the current amplitude,  $I_p$ , and the time,  $t$ , shifted in phase  $\phi$  of the sinusoidal signal:

$$I_{pzt}(t) = I_p \sin(2\pi ft + \phi) \quad (2)$$

The following expression analogous to Ohm's Law allows for the estimation of the impedance of the PZT,  $Z_{pzt(t)}$ , as a function of time,  $t$ :

$$\begin{aligned} Z_{pzt}(t) &= \frac{V_{pzt}(t)}{I_{pzt}(t)} = \frac{V_p \sin(2\pi ft)}{I_p \sin(2\pi ft + \phi)} \\ &= |Z| \frac{\sin(2\pi ft)}{\sin(2\pi ft + \phi)} \end{aligned} \quad (3)$$

The electrical impedance is also expressed in a complex notation by the following well-known Euler's relationship:

$$\exp(j\phi) = \cos\phi + j\sin\phi \quad (4)$$

where  $j = \sqrt{-1}$ .

This way, since the frequency response of the voltage and the current of the PZT are:

$$V_{pzt}(f) = V_p \exp(j\phi) \quad (5)$$

$$I_{pzt}(f) = I_p \exp(j\phi) \quad (6)$$

the frequency response of the electrical impedance  $Z_{pzt(f)}$  is given by the following complex relationships:

$$Z_{pzt}(f) = \frac{V_{pzt}(f)}{I_{pzt}(f)} = R + jX \quad (7a)$$

$$|Z| = \sqrt{R^2 + X^2} \quad (7b)$$

where  $R$  is the real component (conductance) and  $X$  is the imaginary component (susceptance):

$$R = |Z| \cos\phi \quad (8a)$$

$$X = |Z| \sin\phi \quad (8b)$$

The developed SHM system also adopts the following simple circuit. A common signal generator produces an alternate current signal with frequency,  $f$ , and excites a resistor,  $R_f$ , which is connected in series with the PZT transducer. This circuit is an efficient methodology to measure impedance magnitude using the sinusoidal input

voltage signal excitation,  $V_{in(f)}$ , and measuring the peak value,  $V_{p(f)}$ , of the output voltage signal of the PZT. It is also known that under a high frequency sinusoidal voltage signal the PZT behaves more or less as a capacitive system that tends to preserve negligible phase difference between voltage and current output signal. For this reason, the impedance amplitude can be evaluated by the expression:

$$|Z(f)| = \frac{V_p(f)}{I_p(f)} \cong \frac{V_p(f)}{\frac{V_{in}(f)}{|Z(f)| + R_f}} \quad (9)$$

Thus, the peak value  $V_{p(f)}$  is estimated by solving the previous equation as follows (Providakis *et al.* 2016):

$$V_p(f) \cong \frac{|Z(f)|}{|Z(f)| + R_f} V_{in}(f) \quad (10)$$

This simple equation indicates that the output peak voltage signal of the PZT transducer depends on the value of the impedance amplitude and, consequently, is directly related to the structural integrity status of the structure. It also allows for the implementation of rather simple and low-cost monitoring modulus with respect to the traditional complex impedance analysers.

## 2.2 WiAMS device

The developed WiAMS is an integrated SHM method that uses the voltage signal measurements of PZT transducers mounted to the RC structural member using the aforementioned aspect. It includes specially manufactured, portable and autonomous WiAMS devices, one for each PZT transducer that is consisted of multiple custom-made modules (Providakis *et al.* 2014a, 2014b).

A low-cost, credit card sized and lightweight single-board computer Raspberry PI has been implemented as the central control unit of the WiAMS device that communicates and controls the integrated circuit modules of the system using an open source Linux-based operating system. It also packs high computing power by an ARM processor, transfers data without the need of a base station and performs all sort of computing tasks, interfacing various sorts of devices and connecting to the internet via WiFi. Thus, the developed SHM system offers advanced characteristics such as remote control by a terminal emulator, email notifications of impending abnormal states and upload to web databases of the monitoring measurement results. Further, the low-cost of the WiAMS devices allows for synchronized real-time monitoring of a large-scale structure (Providakis *et al.* 2016).

The WiAMS device is connected by two cables to the poles of a PZT patch mounted to the RC structure. The implemented PZT is first excited by a predefined and appropriate range of sinusoidal frequencies which is selected and controlled by the user via the Raspberry PI in order to successfully activate the transducer. The frequency response is generated by the signal generator module, which is then amplified and applied as an input voltage signal,  $V_{in(f)}$ , to the PZT actuator. The peak detector module that is directly connected to the PZT detects its peak voltage response value. Right afterwards, the output voltage versus

frequency response of the PZT patch, which operates at the same time as sensor, is received and recorded by the WiAMS device. Conversely, the output voltage frequency response of the PZT,  $V_{pzt}(f)$ , passes through the peak detector to measure the peak voltage value,  $V_p(f)$ . Then, a custom-made Analog-to-Digital Converter module is used to digitally measure the peak voltage and all the measured data are transferred to Raspberry PI in digital form and stored on it (Providakis *et al.* 2016).

### 3. Testing of the RC frames

The test project of this study includes two large-scale RC frame specimens (one bare and one X-braced) subjected to lateral full cycle deformations.

#### 3.1 Geometrical and reinforcement characteristics

The examined RC frame subassemblages are single-storey, one-bay frames. They are large-scale RC specimens with external dimensions  $3.0 \times 2.4$  m, as shown in Fig. 1. The first specimen is the bare RC frame (un-strengthened frame used as reference specimen) and the second one is the X-braced one (strengthened frame with diagonal X-type steel elements as tension-ties).

The application of diagonal steel braces in the openings of existing RC frames is a popular and a rather easy-to-apply method for the local or global strengthening of RC frame structures that undergo to earthquake excitations. It has also been proven as an effective upgrading technique since it enhances the overall lateral performance improving strength, stiffness and energy dissipation capacity (Massumi and Absalan 2013, Liolios *et al.* 2017, Lian and Su 2017, Li *et al.* 2018.). The lateral response of braced RC frames presents similar favourable characteristics with the seismic performance of masonry infilled RC frames (Karayannis *et al.* 2005, Lima *et al.* 2014, Massumi *et al.* 2015) when compared to the behaviour of bare RC frames. However, the steel braced method is a more feasible strengthening technique since it requires less space and provides flexibility in architectural design since it is a non-invasive and reversible intervention.

The geometrical and the reinforcement characteristics of the RC structural members of the frames are the same and represent a typical old RC moment-resisting frame structure in Greece that has been designed and constructed using past Code provisions without proper seismic requirements. The cross-sectional dimensions of the beam and the columns of the frames are  $200 \times 300$  mm. The longitudinal reinforcing bars of the beam and the columns are  $4\text{Ø}12$  and  $6\text{Ø}14$  (deformed steel bars, diameters in mm), respectively. The transverse reinforcement of all structural members consists of mild steel closed stirrups of 6 mm diameter uniformly distributed throughout their total length and 200 mm spacing ( $\text{Ø}6/200$  mm). Dimensions and reinforcement configuration of the RC structural members that compose both frames are illustrated in Fig. 1.

The steel X-bracing system of the strengthened RC frame includes two rods of St46 structural steel with

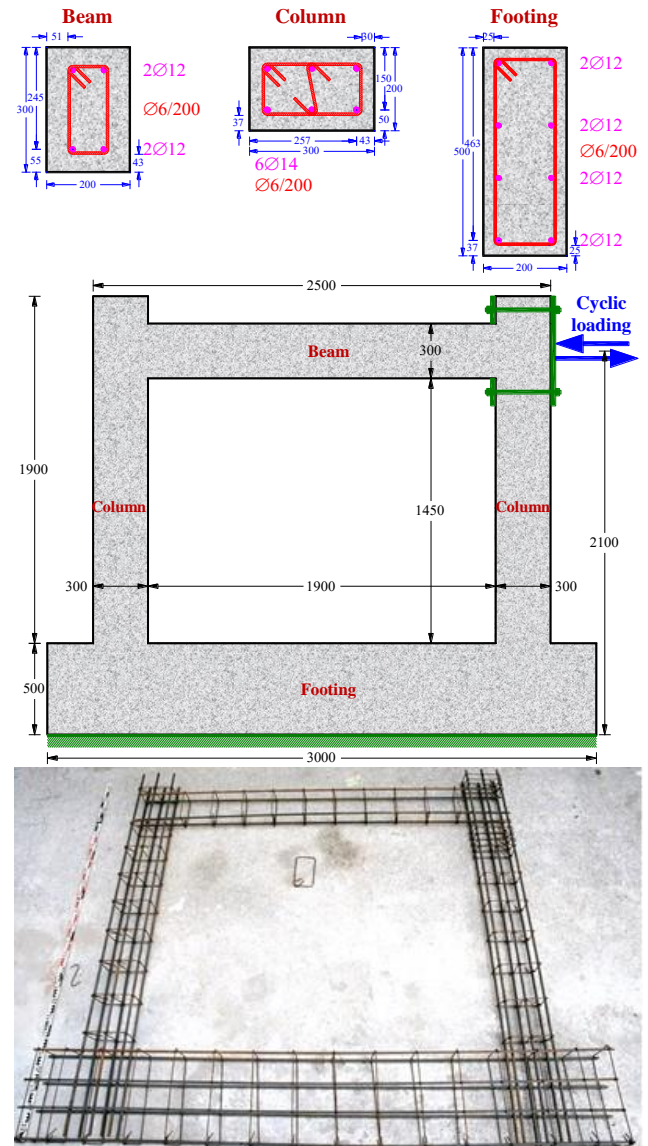
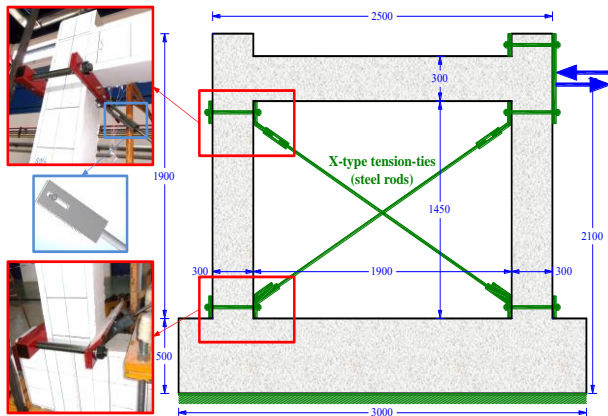


Fig. 1 Dimensions and reinforcement configuration of the structural members of the RC frames

diameter of 16 mm that have placed diagonally inside the RC frame in X-type arrangement as shown in Fig. 2(a). These rods have been connected to the columns of the RC frame very close to the upper and lower joints of the frame using steel brackets and have been installed in order to operate only in tension (see also the detail in Fig. 2(a)).

The shear ratio of the RC columns is low and equal to  $0.925 / 0.30 = 3.1 (> 2.5)$ . Further, the ratio of the column net height to the maximum sectional dimension is  $1.45 / 0.30 = 4.8 (> 3)$ . Although the columns are not strictly defined as “short”, these ratios are low. Further, the columns have wide spacing of stirrups along their entire height and, therefore, their transverse shear reinforcement is rather inadequate for cyclic lateral actions. Thus, all the aforementioned reasons make the columns of the RC frames vulnerable to shear failure during seismic excitations (Karayannis *et al.* 1994, Tsonos 2006, 2009, Chaliotis and Bantilas 2017, Cavaleri *et al.* 2017, Asteris *et al.* 2019).



(a) Characteristics of the X-braced RC frame

(b) Test rig and instrumentation of the cyclic test  
Fig. 2. X-braced RC frame and experimental setup

### 3.2 Test rig of the lateral cyclic loading

The RC frames have been subjected to the same lateral cyclic in-plane displacement-control loading in a rigid RC floor - wall testing area. Test rig and instrumentation are demonstrated in Fig. 2b. The footing of the RC frames was properly fixed to the rigid floor by bolts and nuts in order to prevent slip of the specimen. The load was imposed to the top corner of the RC frames using a double acting servo-controlled hydraulic actuator fixed to the rigid wall of the laboratory with maximum capacity of 500 kN and 500 mm total stroke connected to an intermediate hydraulic control unit to ensure its smooth operation (Liolios *et al.* 2017).

Displacements were measured via a number of digital strain gauges, positioned at different locations on the frame. Linear Variable Differential Transformers (LVDTs) and String Displacement Transducers (SDTs) were used. LVDTs were positioned on the top and bottom corners of the frames to measure the net in-plane horizontal displacements of the frame and on the opposite faces to measure any possible twisting or out-of-plane deformation of each frame. SDTs were positioned on the internal diagonals of the frames to measure the diagonal deformations. SDTs were also diagonally positioned on the upper beam-column joints of the frames to measure the shear deformations of the joint area. All measuring devices were placed in appropriate locations and connected to data logger for digital recording.

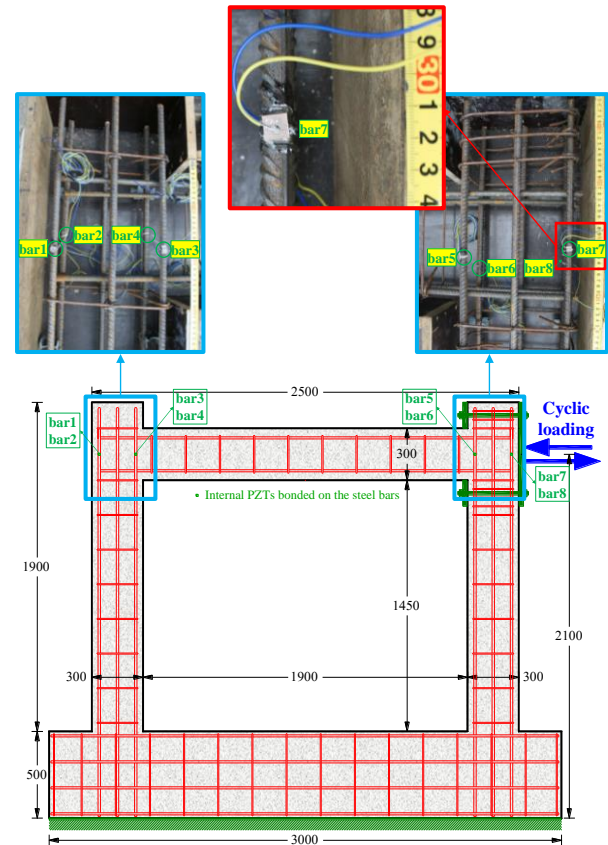


Fig. 3. Locations and installation of the epoxy bonded PZTs on the steel longitudinal reinforcing bars of the columns of the tested RC bare frame

### 3.3 Setup of the developed SHM system

Structural integrity of the tested RC frames has been assessed using the piezoelectric active sensing wireless SHM system (WiAMS) described in section 2. Detection, localization and evaluation of the damages caused due to the imposed quasi-static cyclic loading is achieved using the voltage versus frequency responses of a network of PZT transducers that have measured through WiAMS portable devices.

Thin and small-sized PZT patches with dimensions 10 mm × 10 mm and material mark designation PIC 255 were used. Twenty (20) PZTs have been installed in the first bare frame and twenty-one (21) PZTs in the second X-braced frame as follows:

- Eight (8) PZTs (denoted as “bar1”, “bar2”, etc.) have been epoxy bonded on the surface of the steel reinforcing bars of the columns at locations shown in Figs. 3 and 6(a) for the bare and the X-braced frame, respectively.
- Six (6) PZTs (denoted as “SA1”, “SA2”, etc.) have been embedded inside the concrete mass of each frame specimen as “Smart Aggregates” at locations shown in Figs. 4 and 6(a) for the bare and the X-braced frame, respectively.
- Six (6) PZTs (denoted as “X1”, “X2”, etc.) have been externally epoxy bonded to the concrete surface at the back face of the RC frames at locations shown in Figs. 5

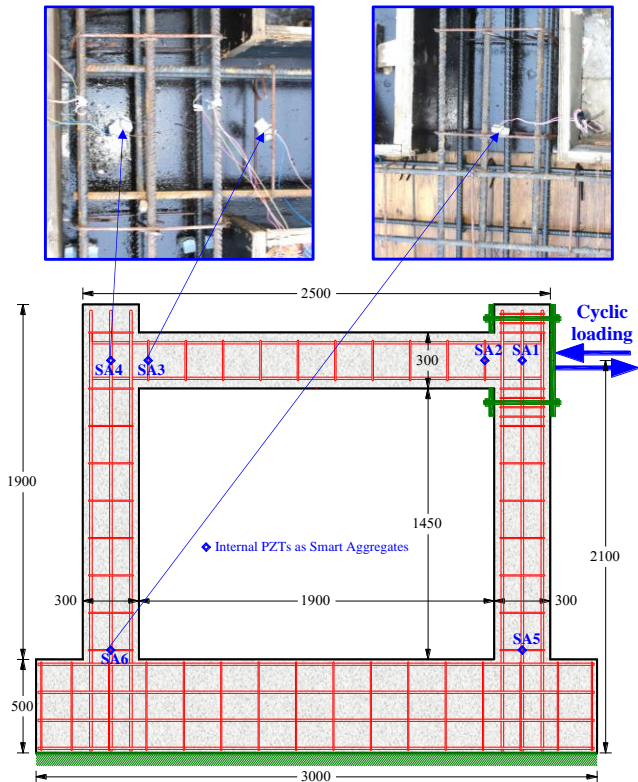


Fig. 4. Locations and installation of the embedded PZTs inside the concrete mass of the RC bare frame as “Smart Aggregates” (SA)

and 6(b) for the bare and the X-braced frame, respectively.

- One (1) PZT (denoted as “X-S”) has been externally epoxy bonded to the diagonal steel rod of the RC X-braced frame at location shown in Fig. 6(b).

It is noted that the PZT transducers in cases (a) and (b) have been internally pre-installed before concrete casting, whereas in case (c) they have been bonded at the beginning of the test.

Epoxy adhesive with a high shear modulus and small thickness has been used to bond the PZTs. A waterproof layer of the epoxy adhesive has also been applied on the top of each PZT in order to protect them during concrete casting and to avoid noise in their signal.

Fig. 7 illustrates the test setup and the block diagram of the implemented wireless SHM system and the small-sized, autonomous and portable WiAMS devices during the cyclic loading procedure of the examined RC frames.

### 3.4 Loading procedure

The horizontal lateral load was imposed at the centroid axis of the beam in a displacement control mode with a rate of 0.2 mm/sec. The applied loading history includes five (5) increasing deformation steps at: (1)  $\pm 1.0$ , (2)  $\pm 3.5$ , (3)  $\pm 12.0$ , (4)  $\pm 22.5$  and (5)  $\pm 45.5$  mm with two equal imposed cycles (A and B) at each step, as presented in Fig. 8. The aforementioned imposed deformations correspond to storey drifts equal to: (1)  $\pm 0.05$ , (2)  $\pm 0.19$ , (3)  $\pm 0.65$ , (4)  $\pm 1.22$  and (5)  $\pm 2.46$  %, respectively.

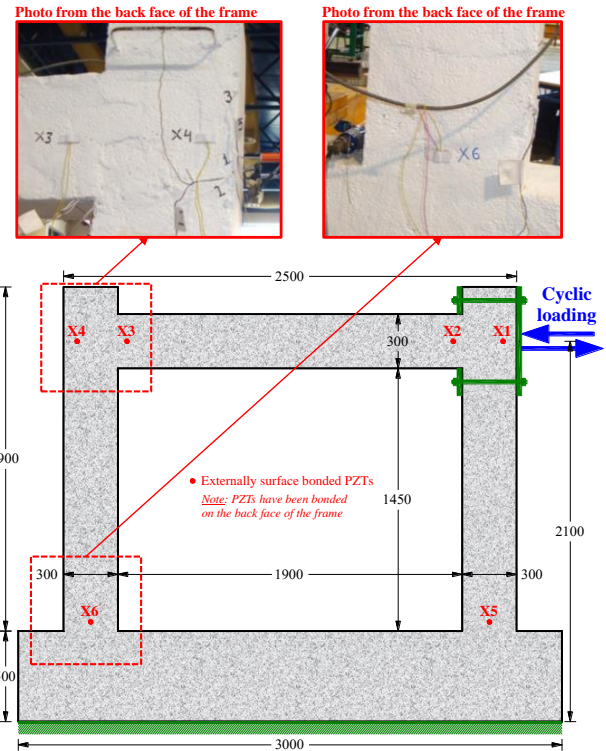


Fig. 5. Locations of the externally epoxy bonded PZTs at the back face of the RC bare frame surface

## 4. Testing of the RC frames

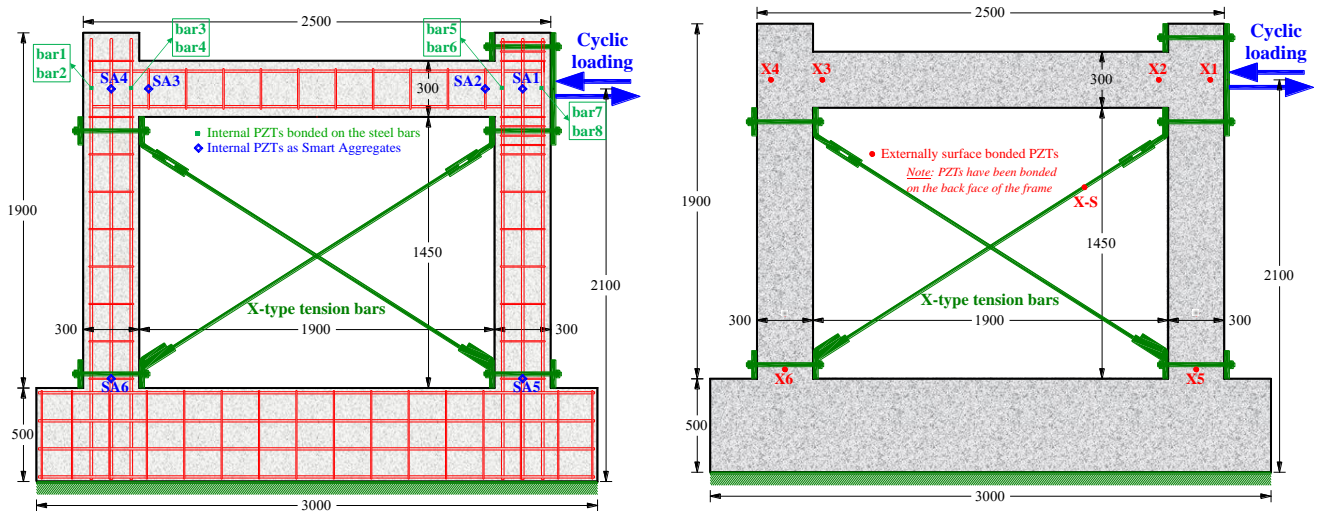
The performance of the tested RC frames under lateral cyclic loading and the ability of the developed SHM system to identify damages due to concrete cracking and steel yielding are detailed discussed in the following subsections.

### 4.1 Bare frame

The hysteretic response of the RC bare frame is presented in Fig. 8 in terms of imposed load versus horizontal displacement. Fig. 9 illustrates four photographs with the cracking patterns of the frame at the end of the 2nd, 3rd, 4th and 5th loading step, which are the examined damage levels. It is noted that the first two loading cycles of the first (1st) loading step developed low stresses, very close to the elastic region of the structural members and therefore the bare frame remained practically undamaged.

At the end of the 2nd loading step only slight and hairline flexural cracks occurred at the conjunctions of the beam and the columns. These cracks formed during loading and closed when unloading (see also Fig. 9(a)). When the RC frame subjected to the 3rd loading step more flexural cracks were propagated from the tip of the existing cracks and several new flexural cracks were generated at new locations and for both lateral loading directions. At the end of the 3rd loading step hairline diagonal cracks observed at both upper beam-column joints area (see also Fig. 9(b)). During the 4th loading step, as the applied load increased new flexural cracks developed, whereas the existing flexural cracks became wider (see also Fig. 9(c)).

The major damage of the RC bare frame occurred at



(a) Internal PZTs: Epoxy bonded on the steel longitudinal reinforcing bars of the columns and embedded inside the concrete mass as “Smart Aggregates” (SA)

(b) External PZTs: Epoxy bonded on the concrete surface

Fig. 6. Locations of the PZTs of the RC X-braced frame

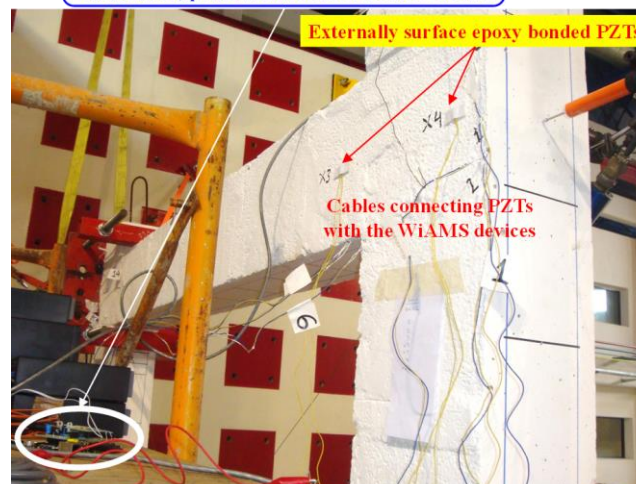
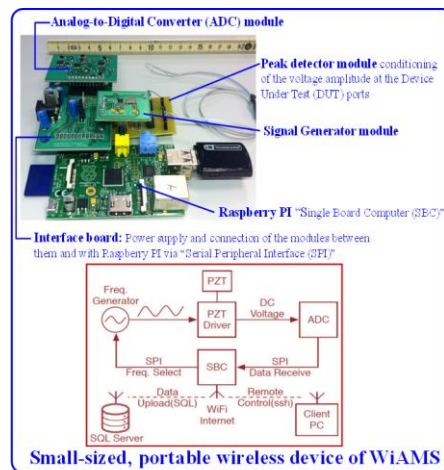


Fig. 7. Test setup of the used SHM system during the cyclic loading procedure of the examined RC frames (view from the top back face of the frame)

displacement approximately 40 mm of the first positive cycle of the 5th loading step due to the development of a severe diagonal crack of the left column that caused brittle

shear failure (see also Fig. 9(d)). It is noted that diagonal cracking was only visible immediately prior to fatal failure which caused a sudden reduction of the load capacity of the

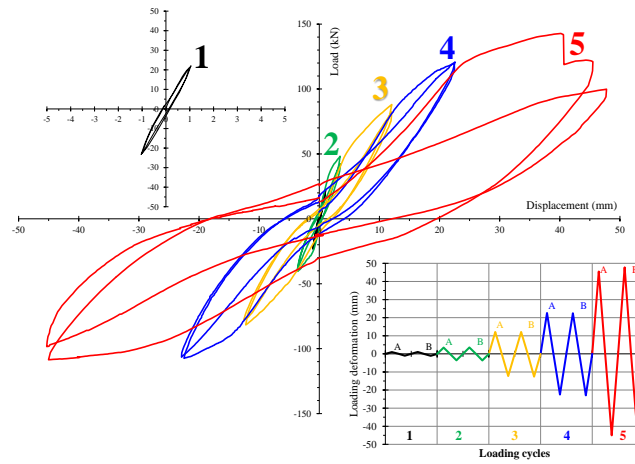
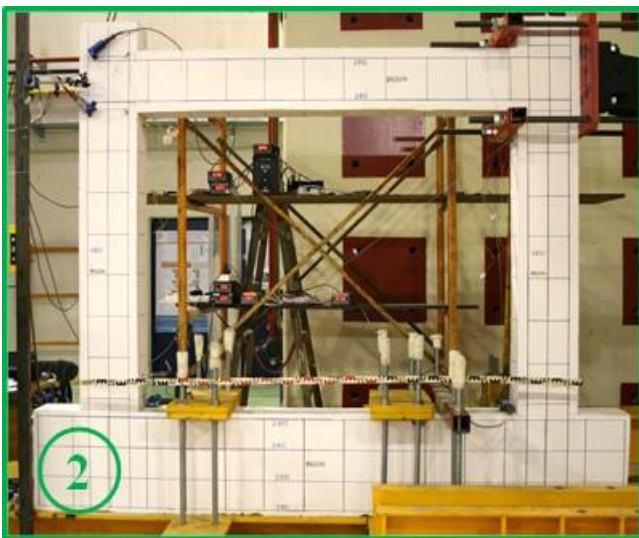
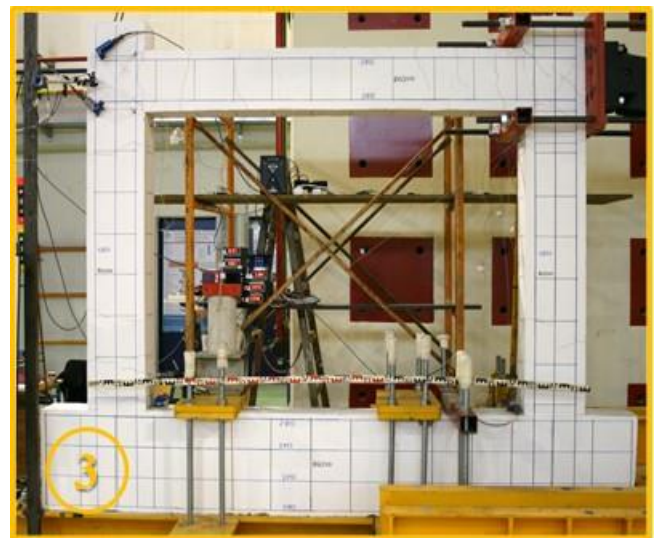


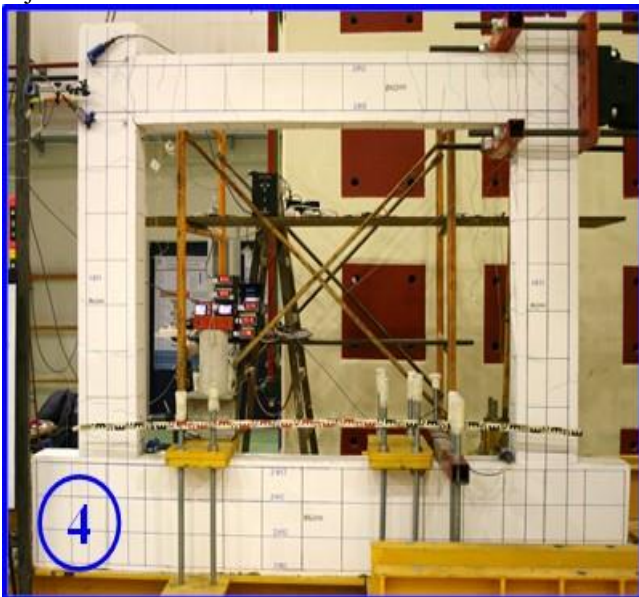
Fig. 8. Hysteretic response of the RC bare frame



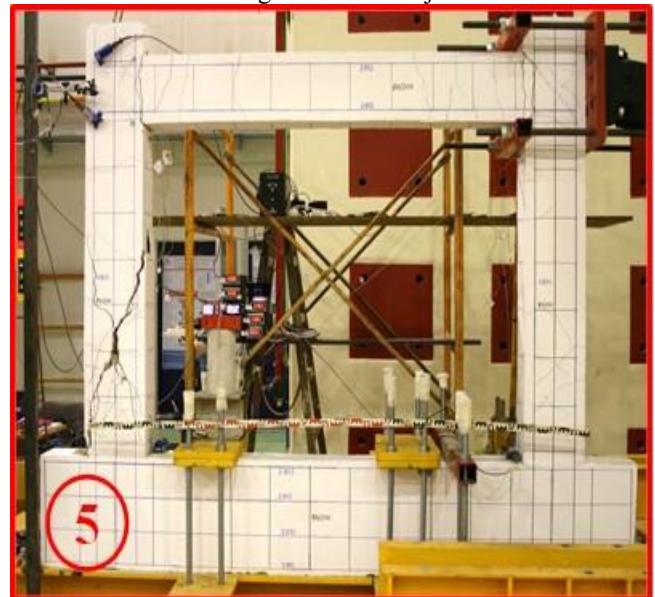
(a) End of loading step 2: Hairline flexural cracks at the beam and conjunctions of the beam and the columns



(b) End of loading step 3: Flexural cracks in beam and columns and hairline diagonal cracks in joints



(c) End of loading step 4: Increased flexural cracking and slight diagonal cracks



(d) End of loading step 5: Failure due to the brittle diagonal cracking of the left column

Fig. 9. Cracking patterns and damages after each loading step - cycle of the RC bare frame

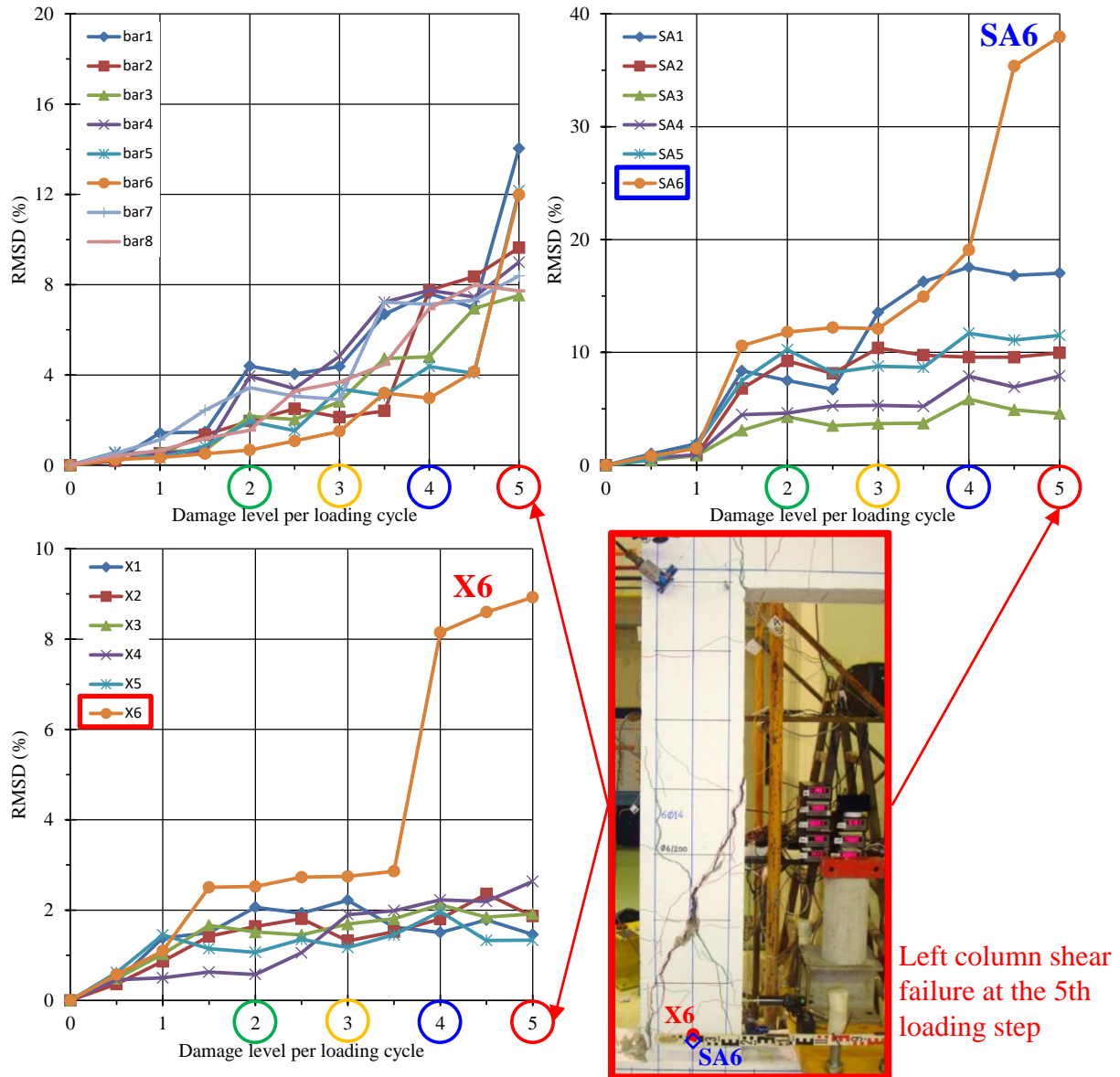


Fig. 10. Values of RMSD index evaluated from the voltage frequency response signals of the PZTs for different level of loading/damage of the RC bare frame

RC bare frame, as shown in the hysteretic response of the frame in Fig. 8. It is obvious that this failure occurred due to the combination of the low height-to-depth ratio of the column that corresponds to a rather short RC structural member and the inadequate transverse reinforcement, which results to low shear resistance, insufficient confinement and low ductility (Armaghani *et al.* 2019).

Fig. 10 presents the results derived from the applied damage detection SHM procedure that is based on the voltage frequency response of the attached PZTs measured by the WiAMS devices during the cyclic test of the bare RC frame. The comparisons of the response of each PZT at the initial healthy state (baseline signal) with the corresponding response at every examined loading level (increasing loading step) that cause an increased damage level provide useful information concerning the structural integrity condition of the examined RC bare frame.

The well-known statistically scalar damage index of the Root Mean Square Deviation (RMSD) is used for the evaluation of the damage severity in the examined RC frame:

$$\text{RMSD} = \sqrt{\frac{\sum_1^N (|V_p(f)|_D - |V_p(f)|_0)^2}{\sum_1^N (|V_p(f)|_0)^2}} \quad (11)$$

where  $|V_p(f)|_0$  and  $|V_p(f)|_D$  are the absolute values of the peak voltage signal measurements of the examined PZT at the healthy “baseline” condition (subscript 0) and at every examined damage level (subscript D) of the RC frame (damage level “1”, “2”, “3”, “4” and “5”), respectively, and  $N$  is the number of the measurements for a frequency index that ranges from 10 kHz to 260 kHz (Voutetaki *et al.* 2016, Chalioris *et al.* 2016).

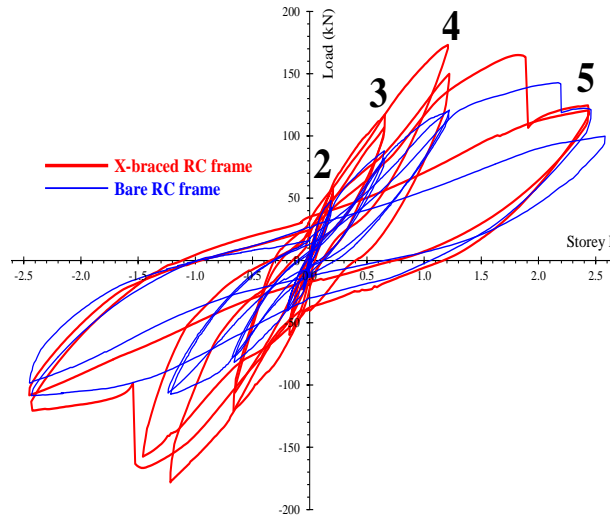


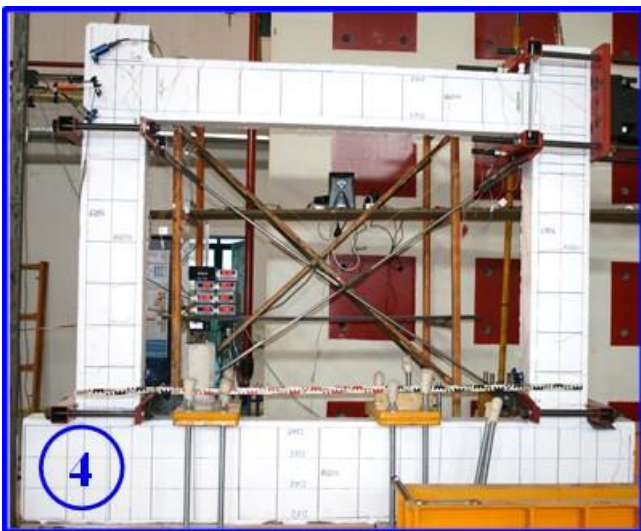
Fig. 11. Comparison of the hysteretic responses of the tested RC frames in terms of load versus storey drift



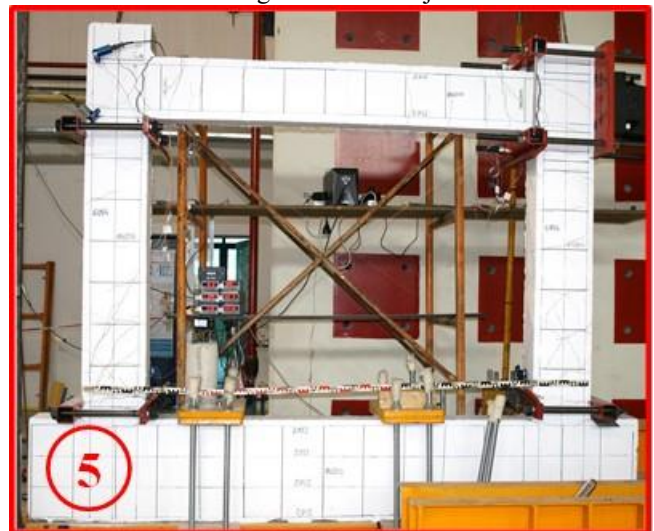
(a) End of loading step 2: Slight hairline flexural cracks in beam



(b) End of loading step 3: Flexural cracks in beam and columns and hairline diagonal cracks in joints



(c) End of loading step 4: Increased flexural cracking mainly in beam



(d) End of loading step 5: Fracture of the steel X-braced rods, hairline diagonal cracks in columns and development of plastic hinges in the beam

Fig. 12. Cracking patterns and damages after each loading step - cycle of the RC X-braced frame

The RMSD values of every PZT at each loading step - cycle are presented in the curves of Fig. 10. Any damage occurred in the tested RC bare frame due to concrete cracking or/and steel yielding causes a change to the voltage signal measurements of the PZTs mounted to the region of the structural member close to the damage. The greater the damage, the greater the change in the voltage signals and, consequently, the greater the absolute value of the RMSD index. This way, RMSD value is used as a feasible damage index that provides a real-time quantitative assessment of damage during a seismic excitation.

The values of RMSD calculated from the voltage frequency response signals of all the twenty (20) PZTs for the five (5) different levels of loading/damage shown in Fig. 10 indicate a consistent increase. This trend confirms the increase of the damage due to the increase of the imposed lateral cyclic deformations (see also the cracking patterns of the RC bare frame in the photographs in Fig. 9).

It is emphasized that the RMSD values of (a) the internally embedded PZT aggregate "SA6" and (b) the externally bonded PZT "X6", which have been installed at the base of the left column (see also Fig. 10) exhibited maximum values and much higher values from the other PZTs during the 5th loading step, right after the development of the fatal shear diagonal cracking that has also been occurred at the base of the left column.

On the contrary, negligible indication of damage derived by the RMSD values of the PZTs located far from the critical cross diagonal cracking of the left column.

Further, promising early warnings of the forthcoming brittle failure are indicated from the high RMSD values of the external PZT "X6" at the 4th loading step, before there is any visible diagonal crack in the base of the left column and before the formation of the critical shear crack during the 5th loading step (see also Figs. 8, 9 and 10).

#### 4.2 X-braced frame

The hysteretic response of the X-braced RC frame is presented and compared with the response of the bare one in Fig. 11 in terms of load versus storey drift ratio. Fig. 12 illustrates four photographs with the cracking patterns of the X-braced frame at the end of the 2nd, 3rd, 4th and 5th loading step. The response in the first two loading cycles of the first (1st) loading step was nearly linearly elastic and the members of the frame remained practically undamaged.

At the end of the 2nd loading step only slight and hairline flexural cracks occurred at the conjunctions of the beam. These hairline cracks formed during loading and closed when unloading (see also Fig. 12(a)). When the RC frame subjected to the 3rd loading step more flexural cracks were propagated from the tip of the existing cracks and several new flexural cracks were generated at new locations and for both lateral loading directions. Further, hairline diagonal cracks observed at both upper beam-column joints area (see also Fig. 12(b)). During the 4th loading step, as the applied load increased new flexural cracks developed, whereas the existing flexural cracks in the beam became wider (see also Fig. 12(c)). It is noted that the application of the steel crossed tension-ties prevented the development of

extensive shear cracking in the columns of the frame and caused a substantial increase of the loading bearing capacity of the strengthened specimen with regard to the cracking and lateral response of the bare one (see also Fig. 11).

The critical damage of the X-braced frame occurred at displacement equal to approximately 35 mm of the first positive cycle of the 5th loading step due to the fracture of the first steel tension tie that caused a sudden reduction of the load (see also Fig. 11). The second tension tie fractured at the right next opposite loading direction of the same cycle. During the 5th loading step two distinct plastic hinges have also been formed in both end regions of the beam, very close to the beam-columns conjunction (see also Fig. 12d). The quite different failure mode of the X-braced frame with regard to the failure of the bare one reveals that the use of the strengthening system succeeded to improve the response by preventing the shear failure of the column.

Fig. 13 presents the values of the RMSD damage index of every PZT at each loading step - cycle. The RMSD values have been calculated from the voltage frequency signals of all the twenty-one (21) PZTs mounted to the X-braced RC frame for the five (5) examined damage levels.

The curves of Fig. 13 indicate that the RMSD index can reflect the damage deterioration quantitatively since RMSD values increase gradually as the damage of the tested frame grows. Further, the RMSD values of the embedded smart piezoelectric aggregates "SA2" and "SA3" which have been installed at the end regions of the beam, very close to the beam-columns conjunction (see also Fig. 10) exhibited higher values from the other PZTs during the 3rd and the 4th loading step, respectively. It is noted that during these loading steps extensive flexural cracking has been developed in these areas and two plastic hinges have finally been formed in both end regions of the beam. Thus, it is concluded that the PZTs located in the vicinity of the severe cracks are more sensitive and register greater changes, or else higher RMSD values, compared to the distant PZTs. Similar remarks are also derived from the results of the PZT "X-S" that has been externally bonded to the diagonal steel tension-tie. The fracture of the tension-tie has been observed at the first cycle of the 5th loading step, whereas steel yield occurred at the 4th loading step. The significant increase of the RMSD value of the PZT "X-S" at this loading step reveals the damage occurred in the steel due to yielding and can be used as a warning of the forthcoming fracture.

Concerning the PZTs that have been epoxy bonded on the surface of the steel reinforcing bars of the columns, since the longitudinal reinforcement of the columns did not yield (in both frames), the RMSD values of these PZTs showed rather slight increases during the tests. These increases are mainly related to the local concrete cracking that has been developed in the regions near the location of these PZTs.

#### 4.3 Effectiveness of the proposed SHM method

Four types of PZT installations have been examined: (a) Epoxy bonded PZT patches on the surface of the steel bars

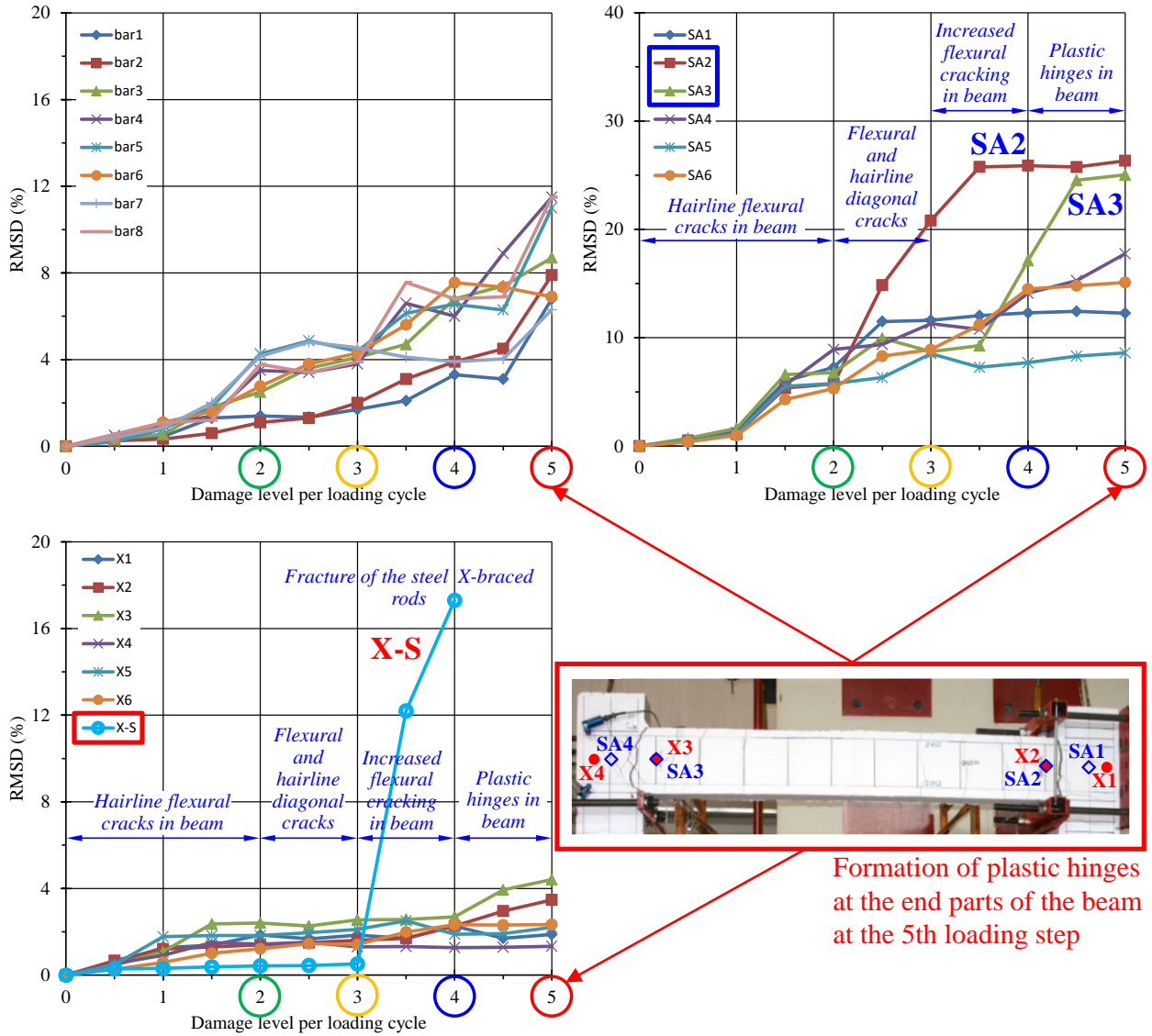


Fig. 13. Values of RMSD index evaluated from the voltage frequency response signals of the PZTs for different level of loading/damage of the RC X-braced frame

of the columns located inside the frame specimens (pre-installed before concrete casting), (b) embedded PZTs inside concrete as “Smart Aggregates (SA)” (pre-installed before concrete casting), (c) externally epoxy bonded PZTs to the concrete surface and (d) externally epoxy bonded PZTs to the diagonal steel rod of the RC X-braced. The experimental results reveal the differences between them. In terms of applicability it is obvious that only externally surface bonded PZT patches can be applied in existing RC structures. Further, the quantitative assessment of damage by integration with the EMA-based RMSD indices of the embedded SA at each cyclic loading step that corresponds to different damage level has been achieved with satisfactory accuracy in the tested RC frames.

On the contrary, the damage sensitivity can hardly be distinguished using the RMSD values of the epoxy bonded PZTs on the surface of the steel bars. This observation could be justified by the fact that steel yielding occurred on the bars of the beams whereas the reinforcing bars of the

columns with the PZT patches remained on the elastic stage.

The effectiveness of the proposed SHM method to damage identification significantly increases by the application of a network of PZT patches arrayed in the critical regions of the structural members of the examined RC frames. Although the voltage signal measurements of individual PZTs in terms of RMSD index values provide slight or even questionable indications of damage, the implementation of a PZT network offer a reliable diagnosis of the severity of damage.

The promising results of this experimental study are focused on the ability of the developed monitoring system to provide early indications of incipient diagonal cracking before the formation of the critical shear failure. Further, the portable, low-cost and self-sensing features of the used WiAMS devices allow to consider the proposed PZT-based SHM technique for practical and wide applications in real-life RC structures in seismically prone regions.

Formation of plastic hinges at the end parts of the beam at the 5th loading step

## 5. Conclusions

An experimental investigation of the effectiveness of a wireless PZT-based monitoring system for the prompt damage diagnosis of seismically deficient RC frames subjected to cyclic deformations has been presented. Two large-scale single-storey single-span RC frames have been tested under lateral cyclic in-plane displacement-control loading. The following conclusions can be drawn within the scope of this study:

- The geometrical and reinforcement characteristics of the RC structural members of the frames represent typical old RC moment-resisting frame structure without consideration of seismic design criteria. The columns of the frames are vulnerable to shear failure under horizontal load due to their low height-to-depth ratio and inadequate transverse reinforcement (stirrups).
- A bare RC frame and a strengthened one using a pair of steel crossed tension-ties (X-bracing) have been examined and hence different crack propagation and failure modes have been observed. The bare frame failed suddenly due to the shear cross diagonal cracks developed in the base of the column, as designed and expected. On the contrary, the X-braced frame exhibited improved cracking and hysteretic response since the columns remained more or less undamaged and two distinct plastic hinges have been formed in both end regions of the beam, very close to the beam-columns conjunction.
- The structural integrity of the examined RC frames has been monitored during cyclic testing using the developed autonomous portable WiAMS devices connected with a network of twenty PZT transducers properly mounted to the structural members of the frame specimens. Damage assessment at five different damage levels has been performed using the voltage signal measurements of each PZT and the calculated RMSD index values. Test results indicated that RMSD index increases gradually with increasing of the damage occurred due to concrete cracking or steel yielding and can effectively quantify the damage severity at various locations and structural conditions.
- PZT transducers located in the vicinity of the intense cracking are more sensitive providing cogent evidence of damage as conducted by the RMSD index values. Further, satisfactory detecting ability on local damage can be achieved by the implementation of a network of PZT patches and the developed EMA-based SHM system. Promising indications of incipient damage identification and prior critical failure warning before any visible sign have also been revealed.

## Acknowledgments

The contribution of the personnel of the Laboratory of Reinforced Concrete and Seismic Design of Structures in Democritus University of Thrace on the experimental procedure and especially the support of N.A. Papadopoulos and G.M. Angeli is sincerely appreciated.

## References

- Ai, D., Luo, H., Wang, C. and Zhu, H. (2018), "Monitoring of the load-induced RC beam structural tension/compression stress and damage using piezoelectric transducers", *Eng. Struct.*, **154**, 38-51. <https://doi.org/10.1016/j.engstruct.2017.10.046>.
- Ai, D., Luo, H. and Zhu, H. (2019), "Numerical and experimental investigation of flexural performance on pre-stressed concrete structures using electromechanical admittance", *Mech. Syst. Signal Proces.*, **128**, 244-265. <https://doi.org/10.1016/j.ymsp.2019.03.046>.
- Ai, D., Zhu, H. and Luo, H. (2016), "Sensitivity of embedded active PZT sensor for concrete structural impact damage detection", *Constr. Build. Mater.*, **111**, 348-57. <https://doi.org/10.1016/j.conbuildmat.2016.02.094>.
- Armaghani, D.J., Hatzigeorgiou, G.D., Karamani, C., Skentou, A., Zoumpoulaki, I. and Asteris, P.G. (2019), "Soft computing-based techniques for concrete beams shear strength", *Proc. Struct. Integr.*, **17**, 924-933. <https://doi.org/10.1016/j.prostr.2019.08.123>.
- Asteris, P.G., Armaghani, D.J., Hatzigeorgiou, G.D. and Karayannis, C.G. (2019), "Predicting the shear strength of reinforced concrete beams using Artificial Neural Networks", *Comput. Concr.*, **24**(5), 469-488. <https://doi.org/10.12989/cac.2019.24.5.469>.
- Bhalla, S. and Soh, C.K. (2004), "High frequency piezoelectric signatures for diagnosis of seismic/blast induced structural damages", *NDT. E. Intl.*, **37**(1), 23-33. <https://doi.org/10.1016/j.ndteint.2003.07.001>.
- Cavaleri, L., Di Trapani, F., Asteris, P.G. and Sarhosis, V. (2017), "Influence of column shear failure on pushover based assessment of masonry infilled reinforced concrete framed structures: A case study", *Soil Dyn. Earthq. Eng.*, **100**, 98-112. <https://doi.org/10.1016/j.soildyn.2017.05.032>.
- Chalioris, C.E. and Bantilas, M.J. (2017), "Shear strength of reinforced concrete beam-column joints with crossed inclined bars", *Eng. Struct.*, **140**, 241-255. <https://doi.org/10.1016/j.engstruct.2017.02.072>.
- Chalioris, C.E., Karayannis, C.G., Angeli, G.M., Papadopoulos, N.A., Favvata, M.J. and Providakis, C.P. (2016), "Applications of smart piezoelectric materials in a wireless admittance monitoring system (WiAMS) to structures - Tests in RC elements", *Case Stud. Constr. Mater.*, **5**, 1-18. <https://doi.org/10.1016/j.cscm.2016.03.003>.
- Chalioris, C.E., Kosmidou, P.M.K. and Papadopoulos, N.A. (2018), "Investigation of a new strengthening technique for RC deep beams using carbon FRP ropes as transverse reinforcements", *Fibers*, **6**(3), 52. <https://doi.org/10.3390/fib6030052>.
- Chalioris, C.E., Papadopoulos, N.A., Angeli, G.M., Karayannis, C.G., Liolios, A.A. and Providakis, C.P. (2015a), "Damage evaluation in shear-critical reinforced concrete beam using piezoelectric transducers as smart aggregates", *Open Eng.*, **5**(1), 373-84. <https://doi.org/10.1515/eng-2015-0046>.
- Chalioris, C.E., Providakis, C.P., Favvata, M.J., Papadopoulos, N.A., Angeli, G.M. and Karayannis, C.G. (2015b), "Experimental application of a wireless earthquake damage monitoring system (WiAMS) using PZT transducers in reinforced concrete beams", *WIT Trans. Built Env.*, **152**, 233-243. doi:10.2495/ERES150191.
- Divsholi, B.S., Yang, Y. and Bing L. (2009), "Monitoring beam-column joint in concrete structures using piezo-impedance sensors", *Adv. Mater. Res.*, **59**, 79-82. <https://doi.org/10.4028/www.scientific.net/AMR.79-82.59>.
- Divsholi, B.S. and Yang, Y. (2014), "Combined embedded and surface-bonded piezoelectric transducers for monitoring of concrete structures", *NDT. E. Intl.*, **65**, 28-34.

- <https://doi.org/10.1016/j.ndteint.2014.03.009>.
- Favvata, M.J. and Karayannis, C.G. (2009), "Influence of exterior joint effect on the inter-story pounding interaction of structures", *Struct. Eng. Mech.*, **33**(2), 113-136. <https://doi.org/10.12989/sem.2009.33.2.113>.
- Ganesh, P. and Murthy, A.R. (2019), "Repair, retrofitting and rehabilitation techniques for strengthening of reinforced concrete beams - A review", *Adv. Concr. Constr.*, **8**(2), 101-117. <https://doi.org/10.12989/acc.2019.8.2.101>.
- Ghafari, E., Yuan, Y., Wu, C., Nantung, T. and Lu, N. (2018), "Evaluation the compressive strength of the cement paste blended with supplementary cementitious materials using a piezoelectric-based sensor", *Constr. Build. Mater.*, **171**, 504-510. <https://doi.org/10.1016/j.conbuildmat.2018.03.165>.
- Gu, H., Moslehy, Y., Sanders, D., Song, G. and Mo, Y.L. (2010), "Multi-functional smart aggregate-based structural health monitoring of circular reinforced concrete columns subjected to seismic excitations", *Smart Mater. Struct.*, **19**, 065026. <https://doi.org/10.1088/0964-1726/19/6/065026>.
- Hou, S., Yu, Y., Zhang, H.B., Mao, X.Q. and Ou, J.P. (2013), "A SA-based wireless seismic stress monitoring system for concrete structures", *Intern J. Distr. Sens. Net.*, **978313**. <https://doi.org/10.1155/2013/978313>.
- Hou, S., Zhang, H.B., Han, X. and Ou, J.P. (2017), "Damage monitoring of the RC frame shaking table test and comparison with FEM results", *Proc. Eng.*, **210**, 393-400. <https://doi.org/10.1016/j.proeng.2017.11.093>.
- Hou, S., Zhang, H.B. and Ou, J.P. (2012), "A PZT-based smart aggregate for compressive seismic stress monitoring", *Smart Mater. Struct.*, **21**, 105035. <https://doi.org/10.1088/0964-1726/21/10/105035>.
- Hu, X., Zhu, H.P. and Wang, D.S. (2014), "A study of concrete slab damage detection based on the electromechanical impedance method", *Sensors*, **14**(10), 19897-19909. <https://doi.org/10.3390/s141019897>.
- Huo, L., Li, X., Li, H., Wang, Z. and Song, G. (2017), "Dynamic modelling of embeddable piezoceramic transducers", *Sensors*, **17**(12), 2801. <https://doi.org/10.3390/s17122801>.
- Kalogeropoulos, G.I. and Tsonos, A.D.G. (2014), "Effectiveness of R/C jacketing of substandard R/C columns with short lap splices", *Struct. Monit. Maint.*, **1**(3), 273-292. <https://doi.org/10.12989/smm.2014.1.3.273>.
- Kalogeropoulos, G.I. and Tsonos, A.-D.G. (2020), "Cyclic performance of RC columns with inadequate lap splices strengthened with CFRP jackets", *Fibers*, **8**(6), 39. <https://doi.org/10.3390/fib8060039>.
- Kalogeropoulos, G.I., Tsonos, A.-D.G., Konstantinidis, D. and Tsetines, S. (2016), "Pre-earthquake and post-earthquake retrofitting of poorly detailed exterior RC beam-to-column joints", *Eng. Struct.*, **12**(7), 1-15. <https://doi.org/10.1016/j.engstruct.2015.11.009>.
- Kang, M.S., An, Y.K. and Kim, D.J. (2018), "Electrical impedance based crack detection of SFRC under varying environmental conditions", *Smart Struct. Syst.*, **22**(1), 1-11. <https://doi.org/10.12989/sss.2018.22.1.001>.
- Karayannis, C.G., Chalioris, C.E., Angeli, G.M., Papadopoulos, N.A., Favvata, M.J. and Providakis, C.P. (2016), "Experimental damage evaluation of reinforced concrete steel bars using piezoelectric sensors", *Constr. Build. Mater.*, **105**, 227-244. <https://doi.org/10.1016/j.conbuildmat.2015.12.019>.
- Karayannis, C.G., Chalioris, C.E., Favvata, M.J. (2013), "Structural upgrading of a 3-storey heritage structure of 1925 in Thessaloniki", *The Proceedings of the 4th ECCOMAS Thematic Conference on Computational Methods in Structural Dynamics and Earthquake Engineering*, Kos Island, Greece, June.
- Karayannis, C.G., Chalioris, C.E. and Sirkelis, G.M. (2008), "Local retrofit of exterior RC beam-column joints using thin RC jackets - An experimental study", *Earthq. Eng. Struct. Dyn.*, **37**(5), 727-46. <https://doi.org/10.1002/eqe.783>.
- Karayannis, C.G., Goliass, E., Chalioris, C.E. (2018), "Local FRP-retrofitting of exterior reinforced concrete beam-column joints under cyclic lateral loading", *The Proceedings of the 16th European Conference on Earthquake Engineering (16ECEE)*, Thessaloniki, Greece.
- Karayannis, C.G., Izzuddin, B.A. and Elnashai, A.S. (1994), "Application of adaptive analysis to reinforced concrete frames", *J. Struct. Eng. ASCE*, **120**(10), 2935-2957. [https://doi.org/10.1061/\(ASCE\)0733-9445\(1994\)120:10\(2935\)](https://doi.org/10.1061/(ASCE)0733-9445(1994)120:10(2935)).
- Karayannis, C.G., Kakaletsis, D.J. and Favvata, M.J. (2005), "Behavior of bare and masonry infilled R/C frames under cyclic loading: Experiments and analysis", *WIT Trans. Built Env.*, **81**. doi:10.2495/ERES050411.
- Karayannis, C.G. and Naoum, M.C. (2018), "Torsional behavior of multistory RC frame structures due to asymmetric seismic interaction", *Eng. Struct.*, **163**, 93-111. <https://doi.org/10.1016/j.engstruct.2018.02.038>.
- Karayannis, C.G. and Sirkelis, G.M. (2002), "Effectiveness of RC beam-column connections strengthening using carbon-FRP jackets", *The Proceedings of the 12th European Conference on Earthquake Engineering*, London, UK, September.
- Karayannis, C.G., Voutetaki, M.E., Chalioris, C.E., Providakis, C.P. and Angeli, G.M. (2015), "Detection of flexural damage stages for RC beams using piezoelectric sensors (PZT)", *Smart Struct. Syst.*, **15**(4), 997-1018. <https://doi.org/10.12989/sss.2015.15.4.997>.
- Kaur, N. and Bhalla, S. (2015), "Combined energy harvesting and structural health monitoring potential of embedded piezo-concrete vibration sensors", *J. Energy Eng. ASCE*, **141**(4). [https://doi.org/10.1061/\(ASCE\)EY.1943-7897.0000224](https://doi.org/10.1061/(ASCE)EY.1943-7897.0000224).
- Kong, Q., Robert, R.H., Silva, P. and Mo, Y.L. (2016), "Cyclic crack monitoring of a reinforced concrete column under simulated pseudo-dynamic loading using piezoceramic-based smart aggregates", *Appl. Sci.*, **6**(11), 341. <https://doi.org/10.3390/app6110341>.
- Kota, S.K., Rama, J.S. and Murthy, A.R. (2019), "Strengthening RC frames subjected to lateral load with Ultra High-Performance fiber reinforced concrete using damage plasticity model", *Earthq. Struct.*, **17**(2), 221-232. <https://doi.org/10.12989/eas.2019.17.2.221>.
- Kuntal, V.S., Chellapandian, M., Prakash, S.S. and Sharma, A. (2020), "Experimental study on the effectiveness of inorganic bonding materials for near-surface mounting shear strengthening of prestressed concrete beams. *Fibers*, **8**(6), 40. <https://doi.org/10.3390/fib8060040>.
- Lagaros, N.D., Fragiadakis, M., Papadrakakis, M. and Tsompanakis, Y. (2006), "Structural optimization: A tool for evaluating seismic design procedures", *Eng. Struct.*, **28**(12), 1623-1633. <https://doi.org/10.1016/j.engstruct.2006.02.014>.
- Laskar, A., Gu, H., Mo, Y.L. and Song, G. (2009), "Progressive collapse of a two-story reinforced concrete frame with embedded smart aggregates", *Smart Mater. Struct.*, **18**(7), 075001. <https://doi.org/10.1088/0964-1726/18/7/075001>.
- Li, S., Wang, C., Li, X., Jian, Z. and Tian, J. (2018), "Seismic behavior of K-type eccentrically braced frames with high strength steel based on PBSO method", *Earthq. Struct.*, **15**(6), 667-685. <https://doi.org/10.12989/eas.2018.15.6.667>.
- Lian, M. and Su, M. (2017), "Shake table test of Y-shaped eccentrically braced frames fabricated with high-strength steel", *Earthq. Struct.*, **12**(5), 501-513. <https://doi.org/10.12989/eas.2017.12.5.501>.
- Lima, C., De Stefano, G. and Martinelli, E. (2014), "Seismic response of masonry infilled RC frames: Practice-oriented models and open issues", *Earthq. Struct.*, **6**(4), 409-436. <https://doi.org/10.12989/eas.2014.6.4.409>.

- Lima, C., Martinelli, E., Macorini, L. and Izzuddin, B.A. (2017), "Modelling beam-to-column joints in seismic analysis of RC frames", *Earthq. Struct.*, **12**(1), 119-133. <https://doi.org/10.12989/eas.2017.12.1.119>.
- Liolios, A., Eftymiopoulos, P., Mergoupis, T., Rizavas, V. and Chalioris, C.E. (2017), "Reinforced concrete frames strengthened by cable elements under cyclic loading: Experimental investigation", *The Proceedings of the 6th International Conference on Computational Methods in Structural Dynamics and Earthquake Engineering*, Rhodes, Greece, June.
- Liu, P., Wang, W., Chen, Y., Feng, X. and Miao, L. (2017), "Concrete damage diagnosis using electromechanical impedance technique", *Constr. Build. Mater.*, **136**, 450-455. <https://doi.org/10.1016/j.conbuildmat.2016.12.173>.
- Massumi, A. and Absalan, M. (2013), "Interaction between bracing system and moment resisting frame in braced RC frames", *Arch. Civil Mech. Eng.*, **13**(2), 260-268. <https://doi.org/10.1016/j.acme.2013.01.004>.
- Massumi, A., Mahboubi, B. and Ameri, M.R. (2015), "Seismic response of RC frame structures strengthened by reinforced masonry infill panels", *Earthq. Struct.*, **8**(6), 1435-1452. <https://doi.org/10.12989/eas.2015.8.6.1435>.
- Na, S. and Lee, H.K. (2012), "A technique for improving the damage detection ability of the electro-mechanical impedance method on concrete structures", *Smart Mater. Struct.*, **21**(8), 085024. <https://doi.org/10.1088/0964-1726/21/8/085024>.
- Narayanan, A. and Subramaniam, K.V.L. (2016), "Experimental evaluation of load-induced damage in concrete from distributed microcracks to localized cracking on electro-mechanical impedance response of bonded PZT", *Constr. Build. Mater.*, **105**, 536-544. <https://doi.org/10.1016/j.conbuildmat.2015.12.148>.
- Park, G., Cudney, H.H. and Inman, D.J. (2000), "Impedance-based health monitoring of civil structural components", *J. Infrastruct. Syst.*, **6**(4), 153-160. [https://doi.org/10.1061/\(ASCE\)1076-0342\(2000\)6:4\(153\)](https://doi.org/10.1061/(ASCE)1076-0342(2000)6:4(153)).
- Providakis, C.P. and Liarakos, E.V. (2014), "Web-based concrete strengthening monitoring using an innovative electromechanical impedance telemetric system and extreme values statistics", *Struct. Contr. Health Monit.*, **21**(9), 1252-1268. <https://doi.org/10.1002/stc.1645>.
- Providakis, C.P., Stefanaki, K.D., Voutetaki, M.E., Tsompanakis, Y. and Stavroulaki, M.E. (2014a), "A near and far-field monitoring technique for damage detection in concrete structures", *Struct. Monit. Maint.*, **1**(2), 159-171. <https://doi.org/10.12989/smm.2014.1.2.159>.
- Providakis, C.P., Stefanaki, K.D., Voutetaki, M.E., Tsompanakis, J. and Stavroulaki, M.E. (2014b), "Damage detection in concrete structures using a simultaneously activated multi-mode PZT active sensing system: numerical modelling", *Struct. Infrastruct. Eng.*, **10**(11), 1451-1468. <https://doi.org/10.1080/15732479.2013.831908>.
- Providakis, C.P., Angeli, G.M., Favvata, M.J., Papadopoulos, N.A., Chalioris, C.E. and Karayannis, C.G. (2014c), "Detection of concrete reinforcement damage using piezoelectric materials-Analytical and experimental study", *Int. J. Civil Environ. Struct. Constr. Archit. Eng.*, **8**(2), 197-205.
- Providakis, C.P., Tsistrakis, S., Voutetaki, M.E., Tsompanakis, Y., Stavroulaki, M.E., Agadakos, J., Kampianakis, E. and Pentas, G. (2016), "An innovative active sensing platform for wireless damage monitoring of concrete structures", *Curr. Smart Mater.*, **1**(1), 49-62. <http://dx.doi.org/10.2174/2405465801666160830155120>.
- Rainieri, C., Fabbrocino, G. and Cosenza, E. (2011), "Integrated seismic early warning and structural health monitoring of critical civil infrastructures in seismically prone areas", *Struct. Health Monit.*, **10**(3), 291-308. <https://doi.org/10.1177/1475921710373296>.
- Sharma, A., Reddy, G.R. and Vaze, K.K. (2012), "Shake table tests on a non-seismically detailed RC frame structure", *Struct. Eng. Mech.*, **41**(1), 1-24. <https://doi.org/10.12989/sem.2012.41.1.001>.
- Shin, S.W. and Oh, T.K. (2009), "Application of electro-mechanical impedance sensing technique for online monitoring of strength development in concrete using smart PZT patches", *Constr. Build. Mater.*, **23**(2), 1185-1188. <https://doi.org/10.1016/j.conbuildmat.2008.02.017>.
- Soh, C.K., Tseng, K.K.-H., Bhalla, S. and Gupta, A. (2000), "Performance of smart piezoceramic patches in health monitoring of a RC bridge", *Smart Mater. Struct.*, **9**(4), 533-542. <https://doi.org/10.1088/0964-1726/9/4/317>.
- Song, G., Gu, H., Mo Y.L., Hsu, T.T.C. and Dhonde, H. (2007), "Concrete structural health monitoring using embedded piezoceramic transducers", *Smart Mater. Struct.*, **16**(4), 959-968. <https://doi.org/10.1088/0964-1726/16/4/003>.
- Song, G., Gu, H. and Mo Y.L. (2008), "Smart aggregates: Multi-functional sensors for concrete structures - A tutorial and a review", *Smart Mater. Struct.*, **17**(3), 033001. <https://doi.org/10.1088/0964-1726/17/3/033001>.
- Talakokula, V., Bhalla, S. and Gupta, A. (2014), "Corrosion assessment of reinforced concrete structures based on equivalent structural parameters using electro-mechanical impedance technique", *Intell. Mater. Syst. Struct.*, **25**(4), 484-500. <https://doi.org/10.1177/1045389X13498317>.
- Talakokula, V., Bhalla, S. and Gupta, A. (2018), "Monitoring early hydration of reinforced concrete structures using structural parameters identified by piezo sensors via electromechanical impedance technique", *Mech. Syst. Signal Proces.*, **99**, 129-141. <https://doi.org/10.1016/j.ymsp.2017.05.042>.
- Talakokula, V. and Bhalla, S. (2015), "Reinforcement corrosion assessment capability of surface bonded and embedded piezo sensors for reinforced concrete structures", *Intell. Mater. Syst. Struct.*, **26**(17), 2304-2313. <https://doi.org/10.1177/1045389X14554133>.
- Tawie, R. and Lee, H.K. (2010), "Piezoelectric-based non-destructive monitoring of hydration of reinforced concrete as an indicator of bond development at the steel-concrete interface", *Cem. Concr. Res.*, **40**(12), 1697-1703. <https://doi.org/10.1016/j.cemconres.2010.08.011>.
- Tian, Z., Huo, L., Gao, W., Li, H. and Song, G. (2017), "Modeling of the attenuation of stress waves in concrete based on the Rayleigh damping model using time-reversal and PZT transducers", *Smart Mater. Struct.*, **26**(10), 105030. <https://doi.org/10.1088/1361-665X/aa80c2>.
- Tsonos, A.-D.G., Kalogeropoulos, G.I., Iakovidis P.E. and Konstantinidis, D. (2017), "Seismic retrofitting of pre-1970 RC bridge columns using innovative jackets", *Int. J. Struct. Eng.*, **8**(2), 133-147. <https://doi.org/10.1504/IJSTRUCTE.2017.084631>.
- Tsonos, A.-D.G. (2006), "Cyclic load behaviour of reinforced concrete beam-column subassemblages designed according to modern codes", *Europ. Earthq. Eng.*, **3**(3), 3-21.
- Tsonos, A.-D.G. (2008), "Effectiveness of CFRP-jackets and RC-jackets in post-earthquake and pre-earthquake retrofitting of beam-column subassemblages", *Eng. Struct.*, **30**(3), 777-793. <https://doi.org/10.1016/j.engstruct.2007.05.008>.
- Tsonos, A.-D.G. (2002), "Seismic repair of reinforced concrete beam-column subassemblages of modern structures by epoxy injection technique", *Struct. Eng. Mech.*, **14**(5), 543-563. <https://doi.org/10.12989/sem.2002.14.5.543>.
- Tsonos, A.-D.G. (2001), "Seismic retrofit of R/C beam-to-column joints using local three-sided jackets", *Europ. Earthq. Eng.*, **15**(1), 48-64.

- Tsonos, A.-D.G. (2009), "Ultra-high-performance fiber reinforced concrete: An innovative solution for strengthening old R/C structures and for improving the FRP strengthening method", *WIT Trans. Eng. Sci.*, **64**, 273-284. doi:10.2495/MC090261.
- Tsonos, A.-D.G. and Stylianidis, K. (2002), "Seismic retrofit of beam-to-column joints with high-strength fiber jackets", *Europ. Earthq. Eng.*, **16**(2), 56-72.
- Vega, D.F., Fernández, C.M., Martínez, P.S. and Velilla, J.P.D. (2019), "System based on piezoelectric sensors for deflection measurement in concrete beams", *Rev. Constr.*, **18**(2), 282-289. doi: 10.7764/RDLC.18.2.282.
- Vougioukas, E., Zeris, C.A. and Kotsovos, M.D. (2005), "Toward safe and efficient use of fiber-reinforced polymer for repair and strengthening of reinforced concrete structures", *ACI Struct. J.*, **102**(4), 525-534. doi:10.14359/14556.
- Voutetaki, M.E., Papadopoulos, N.A., Angeli, G.M. and Providakis, C.P. (2016), "Investigation of a new experimental method for damage assessment of RC beams failing in shear using piezoelectric transducers", *Eng. Struct.*, **114**, 226-40. <https://doi.org/10.1016/j.engstruct.2016.02.014>.
- Wang, D.S., Song, H. and Zhu, H.P. (2013), "Numerical and experimental studies on damage detection of a concrete beam based on PZT admittances and correlation coefficient", *Constr. Build. Mater.*, **49**, 564-574. <https://doi.org/10.1016/j.conbuildmat.2013.08.074>.
- Wang, D.S. and Zhu, H.P. (2011), "Monitoring of the strength gain of concrete using embedded PZT impedance transducer", *Constr. Build. Mater.*, **25**, 3703-3708. <https://doi.org/10.1016/j.conbuildmat.2011.04.020>.
- Xu, B., Zhang, T., Song, G. and Gu, H. (2013), "Active interface debonding detection of a concrete-filled steel tube with piezoelectric technologies using wavelet packet analysis", *Mech. Syst. Signal Proces.*, **36**(1), 7-17. <https://doi.org/10.1016/j.ymsp.2011.07.029>.
- Yang, Y., Divsholi, B.S. and Soh, C.K. (2010), "A reusable PZT transducer for monitoring initial hydration and structural health of concrete", *Sensors*, **10**(5), 5193-5208. <https://doi.org/10.3390/s100505193>.
- Zhang, J., Xu, J., Guan, W. and Du, G. (2018), "Damage detection of concrete-filled square steel tube (CFSST) column joints under cyclic loading using piezoceramic transducers", *Sensors*, **18**(10), 3266. <https://doi.org/10.3390/s18103266>.